B-cell signaling networks reveal a negative prognostic human lymphoma cell subset that emerges during tumor progression

Jonathan M. Irish[a,b], June H. Myklebust[a], Ash A. Alizadeh[a], Roch Houot[a], Jeff P. Sharman[a], Debra K. Czerwinski[a], Garry P. Nolan[b,1], and Ronald Levy[a,1,2]

[a]Department of Medicine, Oncology Division, Stanford University, Stanford, CA 94305; [b]Department of Microbiology and Immunology, Baxter Laboratory of Genetic Pharmacology, Stanford University, Stanford, CA 94305

Human tumors contain populations of both cancerous and host immune cells whose malignant signaling interactions may define each patient's disease trajectory. We used multiplexed phospho-flow cytometry to profile single cells within human follicular lymphoma tumors and discovered a subpopulation of lymphoma cells with impaired B cell antigen receptor (BCR) signaling. The abundance of BCR-insensitive cells in each tumor negatively correlated with overall patient survival. These lymphoma negative prognostic (LNP) cells increased as tumors relapsed following chemotherapy. Loss of antigen receptor expression did not explain the absence of BCR signaling in LNP tumor cells, and other signaling responses were intact in these cells. Furthermore, BCR signaling responses could be reactivated in LNP cells, indicating that BCR signaling is not missing but rather specifically suppressed. LNP cells were also associated with changes to signaling interactions in the tumor microenvironment. Lower IL-7 signaling in tumor infiltrating T cells was observed in tumors with high LNP cell counts. The strength of signaling through T cell mediator of B cell function CD40 also stratified patient survival, particularly for those whose tumors contained few LNP cells. Thus, analysis of cell–cell interactions in heterogeneous primary tumors using signaling network profiles can identify and mechanistically define new populations of rare and clinically significant cells. Both the existence of these LNP cells and their aberrant signaling profiles provide targets for new therapies for follicular lymphoma.

B-cell receptor | follicular lymphoma | phospho-flow cytometry | signaling profile

Signaling governs both intrinsic and extrinsic functions of cells, arbitrating decisions at checkpoints throughout development and directing a cell's behavior as it responds to events in its environment. In cancer, mutations and epigenetic events confer upon cells attributes required for aggressive growth, malignancy, and therapeutic resistance. These changes impact the cell signaling network architecture and create signature signaling profiles that can be associated at the single cell level with clinical features of each patient's disease (1, 2). It is becoming clear that the heterogeneity inherent in tumor cell populations creates a need to understand how diverse populations of tumor cells continuously interact with each other and surrounding nonmalignant cells before and during therapy. Single cell analysis of signaling has significant potential for understanding disease course at these junctures, as cell subpopulations within a primary human tumor—such as tumor initiating stem cells and infiltrating immune cells—can be identified on the basis of surface markers and further distinguished by their phenotypic signaling potential and biological response profiles (3, 4).

Follicular lymphoma (FL) is an indolent human malignancy that is currently incurable in the vast majority of cases, and patient clinical outcomes are markedly heterogeneous. FL is also often a precursor of aggressive lymphoma, such as diffuse large B cell lymphoma (DLBCL), an important cause of disease-related death (5). Understanding biological features that distinguish patients' tumors is critical in developing treatments to improve clinical outcomes. For instance, during FL tumor progression, selection likely expands cancer cell subsets with signaling features that enable cell survival in the context of treatment and immune surveillance (4, 6, 7). It may also be critical to understand how the tumor microenvironment contributes to FL clinical outcomes (8, 9). A singular feature of B cell FL is the B cell receptor (BCR), a complex of proteins poised to activate several attendant downstream signaling pathways and deliver signaling necessary for cell division and survival in lymphoma (10–12). BCR signaling has been implicated in other B cell lymphomas (13–16), and carbohydrate modifications to the BCR may alter signaling interactions of FL cells (17). Because BCR activation can initiate signals resulting in either survival or apoptosis of B cells (18–21), this pathway provides many opportunities for selective pressure to elicit the emergence of lymphoma subsets.

We combined immunophenotyping and potentiated phospho-specific cytometry of cellular responses to provide a detailed individual cell view of signaling networks in both cancer cells and patient immune effector cells. Ultimately, this single-cell view revealed the outgrowth of a subpopulation of lymphoma cells whose signaling profile differed from the bulk tumor in patients with a negative clinical outcome. The network level view allowed visualization of this key population of cells over time in patients' tumors and revealed how signals these cells might expect to see in their microenvironment relate to clinically significant changes in cell signaling networks. The single-cell approach provided for a refined prognostic model based on signaling in a tumor cell subset that stratified overall survival as well as suggested mechanisms by which such tumors escape therapies and the immune system. Notably, although BCR signaling prominently correlated with clinical outcomes, CD40 activation as well as infiltrating T cell signaling attributes were also prognostic, albeit to a lesser degree. This suggests a systems view of tumor biology wherein

multiple elements of intracellular networks as well as intercellular interactions compel clinical outcomes—provoking an approach to FL that accounts for these multiple attributes to inspire new treatment strategies.

Results

Signaling Profiles of Lymphoma B Cells and Tumor-Infiltrating T Cells.

Tumor samples were profiled by a surface immunophenotyping panel and their pathway dependent functional phenotypes were determined by phospho-specific flow cytometry (Fig. 1*A*). Live tumor cells were split for stimulation by signaling inputs and then fixed at given time points to prevent signaling from proceeding. Cells were then permeabilized for intracellular antibody staining and stained by antibody panels that measured per-cell phospho-protein levels and lineage markers for lymphoma B cells, tumor infiltrating T cells, and nontumor B cells.

In FL, tumors contain a large number of lymphoma B cells and a variable but significant amount of nonmalignant tumor-infiltrating T cells (22). Expression of B cell antigen CD20 and T cell antigens CD5 and CD3 distinguished B and T cell populations within FL patient samples (Fig. 1*B*). FL tumors were also characterized by 20 markers of nontumor B cells, natural killer cells, and myeloid lineage cells (*SI Materials and Methods*). Tumor-infiltrating nonmalignant cells other than $CD5^+$ $CD3^+$ T cells were rare. BCR isotype restriction is a hallmark of FL cells, and lymphoma B cells expressed a single Ig light chain isotype (Fig. 1*B*). Detection of the nontumor light chain isotype distinguished rare nonmalignant B cells, (Fig. 1*B*, kappa$^+$ cells). In addition to isotype restriction, a feature of FL is the 14;18 translocation, which results in B cell CLL/lymphoma 2 (BCL2) overexpression (23). BCR light chain isotype restriction and BCL2 overexpression clearly distinguished lymphoma B cell identity.

To profile signaling in B and T cells simultaneously, we developed a panel of 12 stimulation conditions targeting B and T cells and combined this panel with 12 matching phospho-protein readouts. Stimuli included CD40 ligand (CD40L), B cell antigen receptor engagement by $F(ab')_2$ (α-BCR), IL-2, IL-4, IL-7, IL-13, IL-15, IFN type I, and IFN-γ (Fig. 1*B*). Signaling responses were gauged by measuring phosphorylation of the associated phospho-proteins in the signaling network, which included Src family kinases (SFKs), SYK, BTK, BLNK, PLCγ, AKT, ribosomal protein S6 (S6), ERK, p38, STAT1, STAT3, STAT5, STAT6, NF-κB p65, and CBL (Fig. 1*B* and *SI Materials and Methods*). Square color intensity represents fold increase in median phosphorylation of stimulated cells, relative to the level in unstimulated cells (arcsinh scale, $+1.75 \approx 10$-fold). As an additional receptor-independent probe of signaling effectors, phorbol 12-myristate 13-acetate plus ionomycin (PMA + iono) was used to induce calcium flux and activate PKC upstream of ERK and p38 in

B and T cells. These signaling readouts provided a network-level analysis of cell signaling by measuring signal transduction pathways known to play a role in cancer and capturing responses of key cancer-associated effectors for the stimuli in the panel (24–30). An initial panel of 12 stimuli × 12 readouts resulted in 288 signaling measurements per patient when examined in both lymphoma B cells and tumor-infiltrating T cells (Fig. 1). Data management and analysis of signaling profiles was simplified by open-source Cytobank software developed for this project.

In addition to the example signaling profile shown (Fig. 1*B*), 23 FL patients and six healthy donors were initially collected (Fig. S1). For each individual, signaling in lymphoma B cells and tumor-infiltrating T cells was examined first using multidimensional flow cytometry plots and then summarized using the population median, represented in a heat map (Fig. 1*B*). We first examined median signaling in FL because median signaling stratified clinical outcome in our prior studies (1). Signaling features in which no significant activity was observed in tumor or healthy cells appear black in heat maps.

In lymphoma cells, reliable BCR pathway phospho-protein readouts included SFK, SYK, AKT, and ERK (Fig. 1*B* and Fig. S1). In addition to α-BCR, PMA + iono and CD40L stimulated a shared set of phospho-proteins in lymphoma B cells and provided controls for pathway specificity and mechanism, used later. BCR signaling, IL-4, and CD40L play important roles in healthy B cell survival, proliferation, and specialization for antibody production. α-BCR, PMA + iono, CD40L, and IL-4 stimulated phosphorylation of their respective phospho-protein readouts in lymphoma B cells and were selective (Fig. 1*B*).

Overall, signaling in tumor-infiltrating T cells contrasted significantly with signaling in lymphoma B cells. The cytokines IL-2, IL-7, and IL-15 normally stimulate proliferation and specialization of healthy T cells by binding receptors including a shared common γ chain. In tumor-infiltrating T cells, IL-2, IL-7, and IL-15 led to specific phosphorylation of STAT5 (Fig. 1*B* and Fig. S1). This STAT5 phosphorylation was significant, as other signaling responses expected in healthy T cells were absent in tumor-infiltrating T cells (Fig. S1). For example, IL-4 and IL-10 were expected to phosphorylate STAT6 and STAT3, respectively, in all B and T cells, but instead led to only weak phosphorylation in tumor-infiltrating T cells (Fig. 1*B*).

Signaling features were analyzed according to physiological relevance superimposed upon their utility as classifiers of clinical outcome (Fig. S2*A*). From the set of all possible signaling features (input stimuli × phospho-protein readouts × cell types), features that significantly differed among patients were identified (Fig. S2*B*). Those features with no significant differences among FL patients Fig. S2*B*, black bars) were excluded from subsequent analysis and those which remained (Fig. S2*B*, gold bars) were
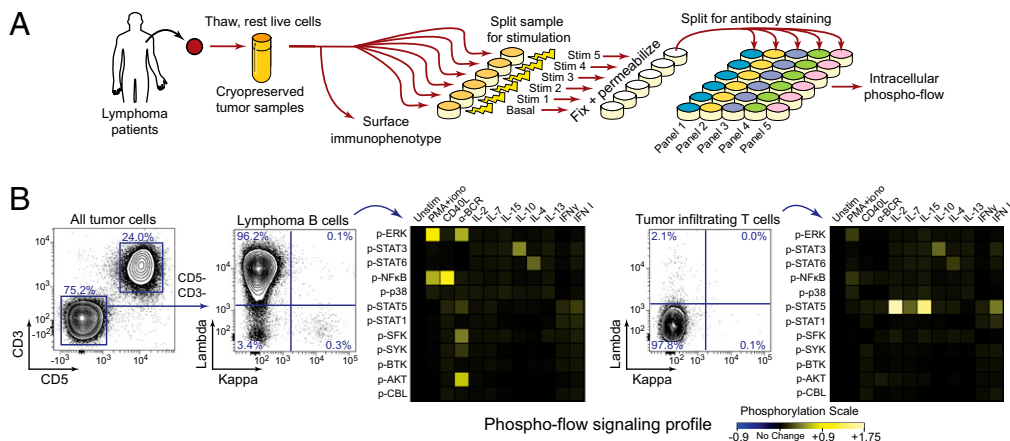
Fig. 1. Signaling profiles of FL B cells and tumor-infiltrating T cells. (*A*) An outline of the phospho-flow assay is shown. A detailed protocol is included in *SI Materials and Methods*. (*B*) Contour plots show gating for $CD3^+$ $CD5^+$ tumor-infiltrating T cells and $CD3^-$ $CD5^-$ lymphoma B cells. Lymphoma B cells were restricted to one Ig heavy and light chain isotype (here, lambda$^+$). Signaling at 12 phospho-proteins was measured following stimulation conditions regulating B and T cells.
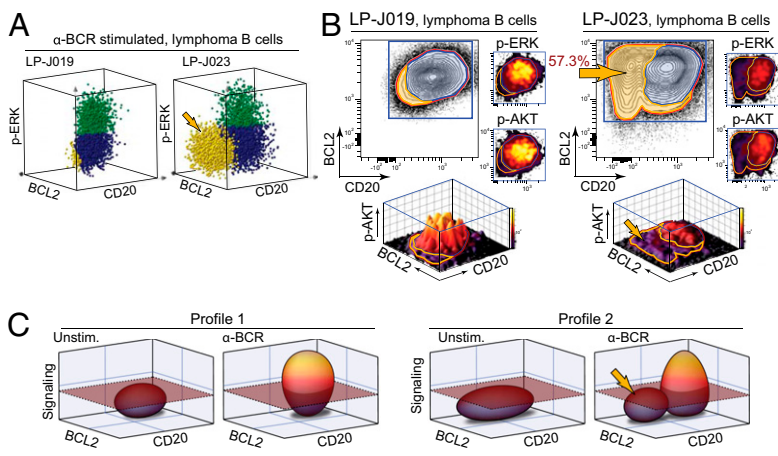
Fig. 2. Identification of a lymphoma cell subpopulation. (*A*) 3D plots of cells measured by flow cytometry show BCL2, CD20, and p-ERK following α-BCR in 4,000 lymphoma B cells from two FL tumors (LP-J019 and LP-J023). (*B*) Cell number (contour plots) and median ERK or AKT phosphorylation following α-BCR (mountain plots) was compared across BCL2 and CD20 in lymphoma B cells from LP-J019 and LP-J023. Flow cytometry plots highlighted a subpopulation of cells within LP-J023 that did not phosphorylate AKT or ERK following α-BCR (gold arrow). (*C*) Models summarize two common FL signaling profiles.

carried forward in the analysis. Notably, basal phosphorylation of signaling proteins in FL B cells was comparable to the level observed in tumor-infiltrating T cells and healthy B and T lymphocytes, and no significant differences in basal signaling were observed across the cohort of lymphoma patients (Fig. S2*B*).

The representation of signaling provided by median fold change summarized signaling in the FL patient cohort and identified elements of lymphoma signaling networks that displayed variation across the cohort (Fig. S2*A*). Although median fold change was useful at a comprehensive level, per-cell analysis was next used to step beyond this summary view of signaling and explore intratumor signaling heterogeneity among individual cells.

BCR Signaling Defined Lymphoma Cell Subpopulation in Human Patients. Per-cell phospho-flow signaling data provided an opportunity to refine the signaling model specifically in the case of α-BCR stimulation. We observed several cases, such as with LP-J023, wherein it was apparent that the lymphoma B cell population was heterogeneous in both α-BCR signaling response and expression of CD20 or BCL2 (Fig. 2*A*) compared with other cohort samples. In the plots shown, tumor cells were grouped into three populations: CD20^{hi} FL cells that responded to α-BCR stimulation (green), CD20^{hi} FL cells that did not respond to α-BCR (blue), and CD20^{lo} FL cells that did not respond to α-BCR stimulation (gold). Although in both LP-J019 and LP-J023 the response to α-BCR stimulation was heterogeneous across the *z* axis (in this case p-ERK), LP-J023 was distinguished from LP-J019 by the population of CD20^{lo} cells lacking a response to α-BCR (Fig. 2, gold arrows) through several downstream kinases and phospho-epitopes (p-ERK is shown, but similar response patterns were observed with p-SFK, p-SYK, and p-AKT; Fig. 2*B* and Fig. S2*C*).

To identify and quantify this distinguishing lymphoma cell subpopulation, the phospho-protein response to α-BCR was plotted as a function of CD20 and BCL2 expression (Fig. 2*B*). In this plot, peak height indicates the degree of α-BCR stimulation of p-AKT or p-ERK. For LP-J023, a low plateau in the CD20^{lo} area (gold outline) and a small peak in the CD20^{hi} area were apparent (Fig. 2*B*). The low plateau indicates a population of cells with no phosphorylation of ERK following α-BCR. The population of cells in this plateau region is the same as the gold-colored population of cells in the 3D plot (Fig. 2*A*). The small peak indicates there was some signaling response to α-BCR. Notably, within the small peak is a mixture of responding and nonresponding CD20^{hi} cells (Fig. 2*A*). In contrast, for LP-J019 we see one roughly symmetrical peak and no significant plateau region because α-BCR responsive and nonresponsive cells have similar CD20 and BCL2 expression. The height of the peak (i.e., degree of phosphorylated protein) for LP-J019 is also higher

than the peak for LP-J023 (Fig. 2*B*) because more of the cells within the population were responsive to stimulation (Fig. 2*A*). Examination of multiple phospho-protein readouts indicated that the cell population that was colored gold in Fig. 2*A* displayed no significant phosphorylation of any of the measured signaling molecules following α-BCR, including SFK, SYK, AKT, and ERK (Fig. 2*B* and Fig. S2*C*).

Patients generally were grouped into one of two classes, termed profile 1 and profile 2 (Fig. 2*C*). Samples may have contained a subpopulation of lymphoma B cells characterized by impaired BCR signaling and differential CD20 or BCL2 expression (Fig. 2*C*). Cells within the subpopulation specific to profile 2 displayed no significant phosphorylation of measured signaling proteins following α-BCR. Hence, the abundance of the lymphoma cell subset specific to profile 2 was included in subsequent comparisons with clinical outcome.

Tumor and Immune Signaling Features Stratify FL Patient Survival. Following the Fig. S2*A* workflow, signaling features were next examined in a training set derived from 56 FL tumor samples collected before any therapy from patients who received uniform initial chemotherapy consisting of a combination of cyclophosphamide, vincristine, and prednisone (CVP) (31). The 56 patients were split into two sets of 28 samples balanced for other features associated with FL clinical outcome, including age, sex, and the clinical prognostic score termed FL International Prognostic Index (FLIPI) (32). The remaining 28 samples formed a testing set that was set aside for validation of significant features identified in the training set.

Signaling features were ranked in terms of how well they stratified overall survival of patients in the training set (Fig. 3*A*). For each stimulation condition in each cell type, all phospho-protein readouts and combinations were examined in the training set (Fig. 3*A*). In cases in which multiple combinations of stimuli and readouts were available, the features that best stratified overall survival are listed. For each feature, patients were divided into groups using the upper and lower 50th percentile of each signaling feature and then overall survival of the two groups was compared by using the Kaplan-Meier method. For signaling features that provided a promising stratification of overall survival, we identified the breakpoint that produced two groups with the best stratification of survival in this training set. In the case of PMA + iono in the tumor B cells, increased p-ERK and decreased p-NFκB p65 each stratified outcome and were thus treated as separate predictors (Fig. 3*A*). Unexpectedly, the IL-7 and IL-15 signaling in the tumor-infiltrating T cells also significantly stratified outcome in the training set as well as most individual attributes of potentiated signaling in the tumor cells themselves (as described later). However, presence of the lymphoma cell subset in profile 2 (Fig. 2, gold arrow) as

demarcated by a combination of surface marker, BCL2 expression and lack of activatable BCR-dependent signaling was considerably better at stratifying clinical outcome than measurements of median signaling (Fig. 3A) by two orders of magnitude in probability.

The signaling profile was then refined to focus on those signaling inputs listed in Fig. 3A. We included additional antibodies against phospho-protein effectors of BCR signaling to provide further insight into midlevel and downstream BCR signaling events. These included phosphorylated B cell linker protein (p-BLNK), 1-phosphatidylinositol-4,5-bisphosphate phosphodiesterase γ (p-PLCγ), and S6. Prior studies highlighted the importance of PLCγ (33) and BLNK (34) in healthy and lymphoma B cells. p-BLNK, p-PLCγ, and p-S6 displayed a large dynamic range of phosphorylation and similar patterns of BCR signaling in lymphoma cell subsets as other readouts, including p-SFK and p-ERK.

Validation of the LNP Subset Model. The lymphoma cell subset in profile 2 provided a negative prognostic in the training set (Fig. 3A). These cells were therefore termed lymphoma negative prognostic (LNP) cells. The LNP cell fraction varied widely among lymphoma specimens (Fig. 3B). Within the training set, we identified a breakpoint in the distribution at approximately 40%, and subdivision according to at least 40% LNP cells stratified patients for overall survival (Fig. 3C). This result was then examined as a hypothesis in the testing set. Researchers were blinded to clinical outcomes until all samples had been scored for percentage of LNP cells. A similar distribution of scores was observed in the testing set (Fig. 3D) and overall survival was again significantly worse for patients with at least 40% LNP cells than for patients with fewer than 40% LNP cells (Fig. 3E). Thus, the testing set of patients validated the LNP cell hypothesis.

Notably, percent LNP cells was independent of other factors known to affect outcome, such as the clinical FLIPI score and its subcomponents, including age (Table S1 and Fig. S3). Summaries of clinical features, LNP cell scores, and biological features for all samples and patients studied are available in Table S2. It might be the case that LNP cell frequency is a continuous variable associated with poor outcome instead of the threshold suggested by an "at least 40% LNP cells" model. Examination of percent LNP cells as a continuous variable in the combined training and testing datasets, shown in Fig. S4, indicated that each 1% increase in LNP cells increased the annual risk of death on average by 2.5%. ($P < 0.000005$; z-score, 4.68). The results

strongly suggest that the LNP subset is not effectively addressed by CVP therapy (Fig. S4B). Taken together, these results indicate that new therapies targeting the LNP cell subset might be needed.

As multiple downstream events from BCR signaling were prognostic of outcome, and because these might vary somewhat from patient to patient, we determined whether an aggregate statistic of BCR signaling gave better stratifying value. Indeed, median BCR signaling stratified outcome in the training set (Fig. 3A) or testing set (Fig. S5). Classification by median BCR signaling was optimal when just considering PLCγ phosphorylation, a particularly robust readout for BCR signaling ($P = 0.005$; Table S3). However, although median BCR signaling was sufficient to stratify overall survival, stratifications by median BCR signaling were weaker than the stratification of overall survival provided by the LNP cell subset model. Approximately 18% of patients were misclassified when using median BCR signaling (5 of 28 patients; Fig. S5). The simpler median-based model performed less well because it could not distinguish cases in which BCR signaling was impaired in a distinct subpopulation from cases in which low BCR signaling was observed in the whole population. Notably, expression of CD20 or BCL2 on their own was not sufficient to stratify patient clinical outcomes (Table S3). The distinctive CD20 or BCL2 expression of LNP cells may represent the expansion of a cell whose CD20 or BCL2 expression is skewed relative to the average expression of each protein in the bulk tumor. In contrast, the association of median BCR signaling with overall survival and the consistent lack of BCR signaling response in the LNP cells suggests that a "hit" to BCR signaling provides a crucial selective advantage that generates the LNP subset.

Emergence and Outgrowth of LNP Cells After Therapy and Progression. The close and continuous association between BCR-insensitive LNP cells and increased risk of death suggested that the LNP cells are closely linked to a patient's poor clinical outcome. If this is the case, paired tumors taken over time from the same individual should relate whether the LNP subset changes in abundance within the tumor and should, in fact, show an increase over time after therapy. Six pairs of serial tumor samples obtained from individual patients were available (Fig. 4A). For each pair, the initial sample was obtained before therapy and the subsequent sample obtained after intervening therapies and disease progression. The percentage of LNP cells within the tumor increased in five of these six cases (Fig. 4A). The fraction of cells with intact
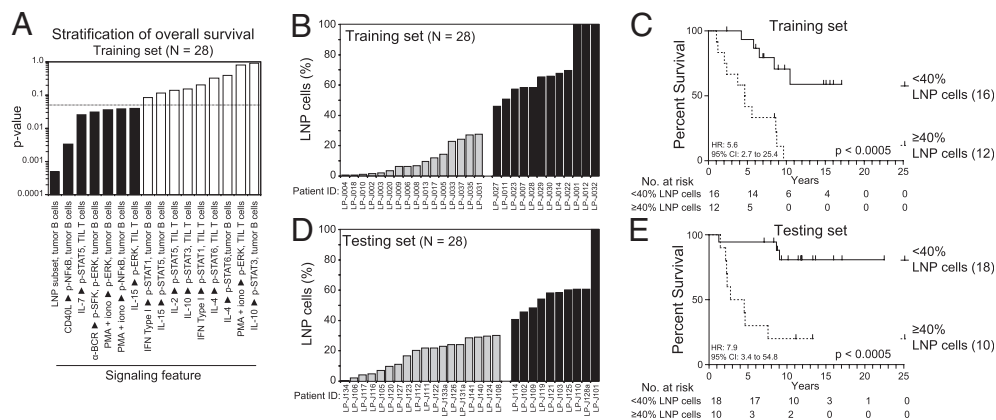
Fig. 3. Presence of LNP cells at diagnosis stratifies overall survival. (A) Significance tests for stratification of overall survival in the training set ($n = 28$) are shown for all FL signaling features. (B) LNP cells were quantified as a percentage of the lymphoma B cells in a training set of 28 FL tumor specimens taken before any therapy (SI Materials and Methods). (C) Overall survival of patients whose tumors contained at least 40% LNP cells and fewer than 40% LNP cells was compared in the training set and found to be significantly lower in the group with at least 40% LNP cells. (D) The LNP cell population was quantified in an independent, balanced testing set of FL patients. (E) The testing set validated the finding from B that patients whose tumor contained at least 40% LNP cells had inferior overall survival. Patients in the training and testing sets were treated with uniform initial chemotherapy.

BCR signaling at each phospho-protein was compared (Fig. 4C and Fig. S6B). At the time of diagnosis, more cells displayed phosphorylation of upstream BCR signaling components, such as SFKs, PLCγ, BLNK, and AKT. Only a small fraction of the tumor cells showed intact phosphorylation of ERK or S6 following α-BCR. In the posttherapy samples, impaired signaling was commensurate for all phospho-protein signaling readouts and BCR-mediated phosphorylation of ERK and S6 had been lost in all the tumor cells (Fig. S6). This is in agreement with the pre-therapy studies in the training study above.

These results indicate that LNP cells have a selective advantage, compared with the bulk tumor B cell population and, together with the direct relationship to risk of death, strongly suggest that the LNP cells are malignant, therapy-insensitive cells. In LNP cells, BCR signaling was compromised at several points throughout the BCR signaling network, including upstream proteins SFK, SYK, BLNK, and PLCγ and downstream proteins ERK, AKT, and p38 (Figs. 2 and 4 and Fig. S2C). This extensive abrogation of BCR signaling suggested a change at the apex of the signaling cascade had occurred. One mechanism for such a change might have been loss of Ig or CD79, the signaling subunit of the B cell antigen receptor. However, subunits of the BCR are not typically lost in FL (35). Furthermore, under the selection pressure of antibody therapy directed against lymphoma BCR idiotype, resistance in FL occurs most often by mutation of the target BCR idiotype rather than loss of BCR expression (36), again in accordance with the view that some aspect of a functional BCR signaling complex is required for lymphoma cell survival, similar to the requirement in mature healthy B cells (18, 19).

We determined Ig heavy chain, Ig light chain, and CD79β expression over time in the paired samples and found that expression did not typically decrease, despite increases in LNP cells (Fig. 4 and Fig. S6). For example, LP-J039 maintained equivalent levels of per-cell expression of Ig whereas the LNP cell subset increased in abundance (Fig. 4). While in some cases, LNP cells displayed lower expression of tumor isotype heavy chain, overall, heavy chain expression did not correlate with the prevalence of LNP cells ($r^2 = 0.31$). Thus, lower antigen receptor subunit expression was not sufficient to explain impaired BCR signaling in LNP cells. A more complete explanation for impaired BCR signaling was needed for the majority of cases in which antigen receptor expression was preserved. Notably, the Ig heavy and light chain isotype of the LNP cells was shared with the other lymphoma B cells for all studied lymphoma cases, and did not change over time in the paired samples examined. This observation suggests that, in addition to the requirement for a functional BCR, LNP cells likely share a common clonal origin with the bulk tumor population.

Having ruled out loss of BCR as a simple explanation for the BCR-insensitive LNP cell phenotype, we next examined the biochemistry of this pathway through further study of the heterogeneous primary lymphoma tumor specimens. Strikingly, stimulation of lymphoma cells by CD40L or PMA + iono bypassed the apparent BCR signaling defect and activated p38, NFκB, and ERK in LNP cells (Fig. 5). In the representative example shown, more than 40% of the lymphoma B cells displayed no phosphorylation of ERK, p38, NF-κB, or any other phospho-protein following α-BCR and were thus considered LNP cells (Fig. 5, gold arrows). In contrast, stimulation of the same tumor specimen by PMA + iono or CD40L led to phosphorylation of ERK, p38, and NF-κB in both the LNP cell population and the remainder of the tumor (Fig. 5, blue arrows), indicating that through alternative pathways this signaling axis could be activated. In particular, phosphorylation of NFκB was especially robust and took place in all tumor cell subsets. These results indicated that BCR signaling was specifically impaired in LNP cells and localized the signaling change to membrane-proximal components of the pathway upstream of PKC (Fig. 5).
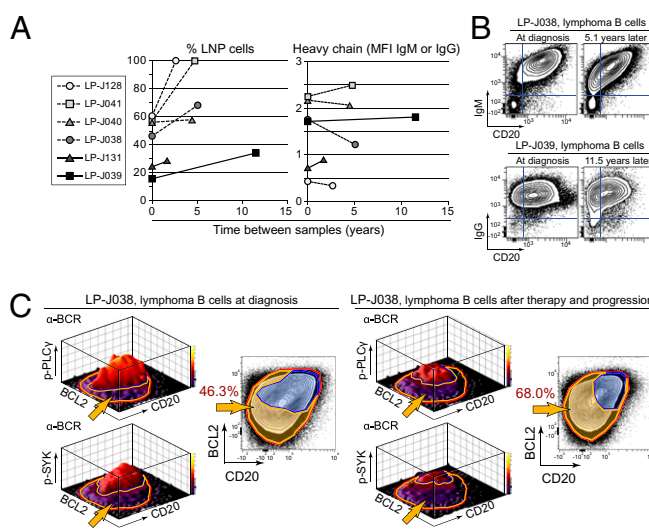
Fig. 4. BCR-insensitive LNP cells increase in abundance after therapy and progression. (A) Percent LNP cells and expression of Ig heavy chain was examined over time in paired samples. Four samples contained at least 40% LNP cells before therapy (dashed lines). (B) Expression of tumor isotype heavy chain and CD20 is shown for samples taken before therapy and after therapy for two patients from A. (C) Changes in the signaling profile of patient LP-J039 over time are shown with flow cytometry contour plots and mountain plots that compare PLCγ and SYK phosphorylation across BCL2 and CD20 following α-BCR stimulation.

Phosphatase Inactivation Reverses the BCR Insensitive Phenotype of LNP Cells. Potential mechanisms of lowering BCR signaling responses in LNP cells might include high constitutive signaling, increased negative regulation, or loss-of-function mutation of an "upstream" kinase, such as SYK or SFK. Differences in basal phosphorylation were small within lymphoma B cell subpopulations and between patients, compared with differences in BCR signaling response (Fig. 6B). This result suggested suppression of signaling in FL occurred through loss of kinase function or increased negative regulation.

When the pattern of signaling in LNP cells was mapped onto a network diagram (Fig. S6), it suggested one explanation for impaired BCR signaling would be increased upstream regulation of signaling. This hypothesis is consistent with the observation that signals that bypass upstream negative regulation of BCR signaling were intact within the LNP cell subset (Fig. 5). If an increase in negative regulation was responsible for impaired BCR signaling in LNP cells, this signaling defect might be reversed by inhibiting tyrosine phosphatases that fine-tune BCR signaling, such as CD45, CD22-associated SHP-1, or PTPROt (22, 37–40). In contrast, if BCR signaling were impaired through loss of kinase function, signaling in LNP cells would not be restored by phosphatase inhibition. Classically, phosphatases that control antigen receptor signaling have been inhibited by the strong oxidant pervanadate or the mechanistically similar milder oxidant H_2O_2 (38). Healthy B cells naturally produce H_2O_2 to control the strength of antigen receptor signaling (39). We have previously used H_2O_2 as a reversible method of inhibiting phosphatases and potentially other molecules that control BCR signaling in healthy B cells (37), so we determined whether signaling in LNP cells could be restored by engaging the BCR in the presence of H_2O_2 (Fig. 6). As an additional control, we used the SYK inhibitor R406 (13, 41) in these experiments.

Strikingly, inhibition of BCR signaling in the LNP cell subset was significantly reversed when BCR was engaged in the presence of H_2O_2 (Fig. 6 A and B). Phosphorylation of ERK and p38 following α-BCR and H_2O_2 was blocked by the SYK inhibitor R406 (Fig. 6 C and D)—thus, mapping the inhibitory effect

upstream of SYK. In contrast, PKC mediated phosphorylation of ERK in response to PMA was unaffected by R406 (Fig. S6). In this experimental series, activation of PKC signaling again served as a positive control, as PKC activity is independent of SYK activation (i.e., PKC is "downstream" from SYK in the BCR signaling network, as shown in Fig. 5). H_2O_2 alone triggers no significant signaling in FL (22). Stimulation by α-BCR and H_2O_2 triggered signaling in LNP cells that was sustained long after the initial stimulation (Fig. 6D and Fig. S2C). We can therefore conclude that BCR mediated SYK-dependent phosphorylation of ERK and p38 could be reactivated in the LNP cell subset, indicating that the framework for BCR-dependent signaling remained intact in these cells.

Taken together, these results indicate that BCR signaling was not permanently lost (Figs. 5 and 6), kinetically delayed (Fig. S2C), or fixed at a high constitutive level in LNP cells (Fig. 6B and Figs. S1 and S2). BCR signaling responses in LNP cells were specifically attenuated, in contrast to PMA and CD40L signaling responses (Fig. 5), and this attenuation was reversible (Fig. 6), indicating BCR signaling molecules are intact in the BCR-insensitive population.

Intercellular CD40 Signaling and Tumor-Infiltrating T Cells as Arbitrators of Disease Status. Additional factors other than BCR signaling are likely to drive the aggressiveness of tumor growth. For instance, B cell costimulatory molecules are important for B cell maintenance and activate critical signaling for proliferation and functional specialization. In addition, the microenvironment of the tumor—composed of stromal and immune cells that support B cell survival through provision of ligands or growth niches—is likely to modulate tumor progression (8).

The CD40 receptor interaction with T helper cells via CD154 (CD40 ligand) is a known key costimulatory event in B cell survival and class switch (42). CD40 signaling can lower the threshold for antigen responses and modulate the resulting signal (43, 44), and downstream effector signaling pathways are shared between BCR and CD40 (Fig. 5). As shown in Fig. 3A, CD40L mediated NF-κB phosphorylation was a highly predictive signaling feature related to outcome in the training set, and it might be expected that changes to CD40 signaling were related to changes in BCR signaling in the LNP cell subset. However, when the combined training and testing sets of patients were stratified according to the LNP cell model, it

was surprisingly apparent that the predictive power of CD40L was restricted to those cases that lack a significant LNP cell subset (Fig. S3). CD40L signaling did not stratify survival for cases with at least 40% LNP cells, whereas it did stratify survival for patients in the with fewer than 40% LNP cells ($P = 0.05$). Notably, there was no direct relationship between the degree of CD40 signaling and the percentage of LNP cells ($r^2 < 0.1$), although there were fewer cases with at least 40% LNP cells that displayed strong CD40 signaling (Fig. S3).

Combined with the result that CD40 signaling was intact within the BCR-insensitive LNP cell subset (Fig. 5), these data provided further evidence that altered CD40 signaling might support tumor maintenance in patients wherein outcome was not determined by LNP levels alone. Thus, although CD40 signaling was not as powerful a prognostic indicator as LNP cells, CD40 signaling provided a potential differential diagnostic via a binary decision tree for those patients whose tumor did not contain a significant LNP cell population and suggested that, within this patient cohort, additional regulatory events acting upon CD40 signaling might complicate clinical outcomes.

As CD40L is expressed on T cells, it could be that altered function of T cells in these patients was additionally stratifying in the same population of patients as CD40 ligand–dependent activation. As shown in Fig. S3, indeed T cell signaling through IL-7 activation of STAT5 significantly stratified outcomes. However, unlike CD40 signaling, IL-7 was not independent of the LNP cell subset (Fig. S3). This relationship between LNP cells and defective IL-7 signaling in tumor-infiltrating T cells suggests it will be of interest in future studies to investigate whether development of the LNP cell subset affects signaling in infiltrating T cells or other tumor microenvironment cells.

Discussion

This study identifies a negative prognostic FL cell subset with impaired BCR signaling in human lymphoma patients. Identification of the LNP cell subset enabled us to track the expansion of these cells over time following successive therapies and tumor progression, showing that LNP cells have a survival or proliferative advantage. In accord with this pattern of expansion, the LNP subset's abundance was negatively associated with patient survival. These results reveal that, as the tumor grows, cancer cell subsets diverge under selective pressure and competing subpopulations arise that can be visualized by distinct patterns of signaling. Interrogating or perturbing cells with an input stimulus and following induced phosphorylation was especially revealing, as a key feature of this lymphoma population was the specific suppression of BCR signaling responses. Thus, LNP cells would have been overlooked in analysis of surface markers or basal signaling alone, underscoring the value of surveying the function of activated or perturbed signaling pathways rather than homeostatic states of such pathways.

The variable presence of LNP cells at diagnosis informs us about the fundamental biology of the malignancy and may explain why FL patient clinical outcomes are so diverse. Going forward, of significant interest would be therapies that target and kill LNP cells. A uniform feature of LNP cells in those patients with poor outcomes was suppressed antigen receptor signaling (Figs. 5 and 6). However, this lack of BCR signaling could be overcome (Figs. 5 and 6). As in previous studies of FL (22), our results here showed a consistent lack of tonic BCR signaling in FL, both in LNP cells and in the bulk tumor (Fig. 6 B–D and Figs. S1 and S2). Tonic BCR signaling has been previously observed for DLBCL (34, 40). Selective pressure for BCR may still exist in vivo, as BCR expression was maintained on LNP cells (Fig. 4).

A simplified version of the LNP cell model could now be used in early-phase clinical trials to stratify patient risk, identify patients who might benefit from the trial, balance treatment arms, and measure changes in the LNP cells over time as a cor-
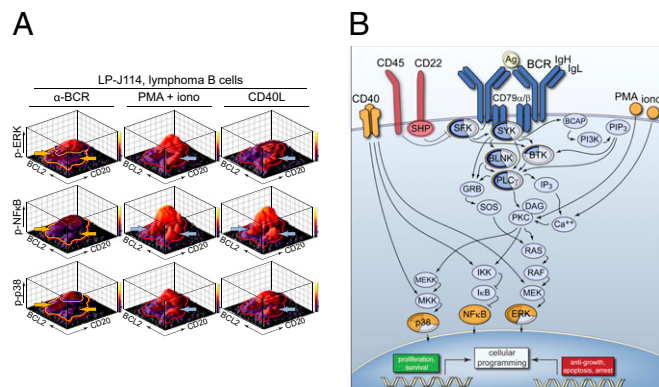
Fig. 5. Signaling proximal to the antigen receptor is specifically impaired in LNP cells. (A) Flow cytometry mountain plots compare phosphorylation of ERK, NF-κB, and p38 across BCL2 and CD20 following α-BCR, PMA + iono, and CD40L. LNP cells (gold arrows), by definition, did not display phosphorylation following α-BCR. Following stimulation with PMA + iono or CD40L, phosphorylation of the same BCR pathway proteins was measured in LNP cells. (B) A signaling network model graphs the results for all measured phospho-proteins. Pie shading indicates the percentage of lymphoma B cells in which phosphorylation of that protein was observed following α-BCR (blue) or PMA + iono or CD40L (orange).
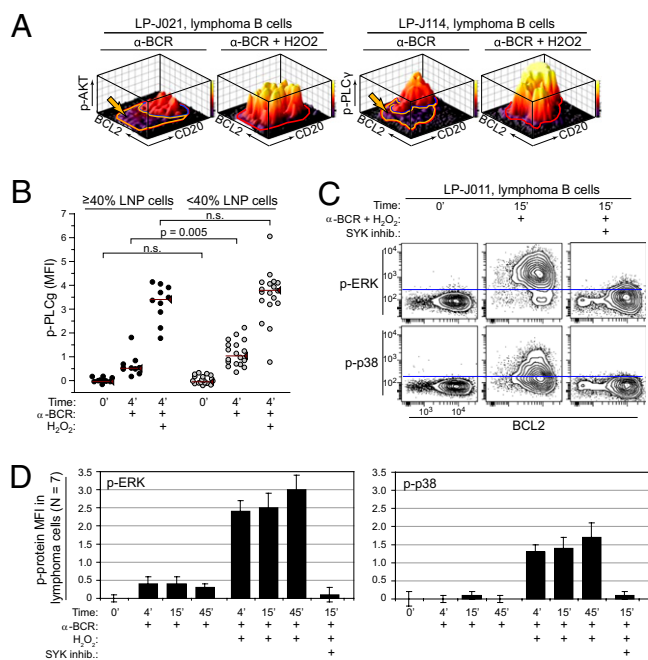
Fig. 6. Impaired BCR signaling in LNP cells is reversed by phosphatase inhibition. (*A*) Mountain flow cytometry plots compare phosphorylation of AKT and PLCγ across BCL2 and CD20 within lymphoma B cells from two tumors that contained LNP cells. Cells were stimulated with α-BCR alone or by α-BCR + H$_2$O$_2$. (*B*) Median basal and BCR-mediated phosphorylation of PLCγ was measured in all lymphoma B cells from patient samples with and without at least 40% LNP cells. No significant difference in basal signaling was observed. Following α-BCR, samples containing at least 40% LNP cells showed significantly lower phosphorylation of PLCγ ($P = 0.005$). This difference between patient groups was eliminated when samples were stimulated by α-BCR + H$_2$O$_2$. (*C*) Contour plots compare phosphorylation of ERK and p38 and expression of BCL2 in lymphoma B cells in the unstimulated basal state, following α-BCR + H$_2$O$_2$, and following 30 min of preincubation with SYK inhibitor R406 before α-BCR + H$_2$O$_2$ stimulation (LP-J011). R406 was used at 2.5 μM to block signaling induced by α-BCR + H$_2$O$_2$ and demonstrate that H$_2$O$_2$ specifically potentiated SYK dependent BCR-mediated signaling. (*D*) Median fluorescence intensity of phosphorylated ERK and phosphorylated p38 is shown for lymphoma B cells from seven cases of FL. Signaling was measured at 4, 15, and 45 min following α-BCR, α-BCR + H$_2$O$_2$, and α-BCR + H$_2$O$_2$ + R406, as in *C*.

ollary end point. Detection of LNP cells could be simplified greatly in future studies because LNP cells are defined as negative for all phospho-protein readouts and phospho-protein readouts can be combined for measurement on a single cytometer channel. Thus, the assay shown here might be simplified to a test that could be conducted in a few hours using standard two-laser four-color flow cytometers found in most hospitals and research facilities. The CVP chemotherapy used during the time these samples were collected is no longer the standard of care. The monoclonal antibody rituximab (45) is now used with current chemotherapy strategies (46, 47). CD20, the rituximab target, tends to be underexpressed on the LNP cells (Fig. 2), and studies of DLBCL recently suggested that low CD20 correlates with inferior outcome (48). Although detection of LNP cells for routine patient decision making must await a validation trial in rituximab-treated patients, these reasons suggest the correlation of LNP cells to clinical outcome will prove robust. The work presented here focuses attention on how this signaling subset can most readily be used as a prognostic tool to guide individualized decisions in FL patient care, such as the decision to "watch and wait" or treat the disease.

The question now arises as to the relationship between the LNP cells and the bulk tumor. The tumor might originate as a homogeneous population of cells and, in accordance with an acquired features model (6), undergo mutation that creates an expansive

LNP cell subclone. Alternatively, the cancer might originate as a small population of LNP cells that produce, through asymmetric cell division or differentiation, the other populations of lymphoma B cells. Over time, immune surveillance and therapy might not eliminate LNP cells, or the LNP cells could be more prone or receptive to mutational events. In this latter model, LNP cells could be considered a cancer stem cell (3, 4). It is likely that LNP cells and other lymphoma B cell populations possess genetic indicators that would shed light on their evolutionary history and perhaps indicate whether one population evolves to become independent of antigenic signals (49–51). CD20 expression was lower on LNP cells compared with other BCR-responsive lymphoma B cells within the same sample, and LNP cells appeared to have restructured their dependence on antigen receptor. Lack of CD20 expression and differences in BCR dependence distinguish both early B lineage cells and terminally differentiated plasma cells from mature B cells. It would be of significant interest in subsequent studies to genotype sorted lymphoma subpopulations and determine whether LNP cells are clonal parents or daughters of the BCR-responsive cells that predominate at early diagnosis.

Regardless of what model ultimately explains the origin of the LNP cells, it is clear that the LNP cells must be eliminated for therapy to be more effective. To clinically address such intratumor signaling heterogeneity, therapies with new mechanisms of action will need to be combined with existing modalities. Potentiated single cell analysis of signaling responses proves here to be a valuable approach to delineate cells that should be acted upon during clinical trials of such therapies, simultaneously linking diagnostic utility to therapeutic action. As is becoming clear with other cancer classes, a combination of therapy modalities will likely be most effective against the heterogeneous populations of lymphoma cells found within each patient's tumor.

Materials and Methods

FL tumor samples were acquired before any therapy from newly diagnosed patients. All patients received the same initial therapy of CVP (31) according to our standard institutional protocol, and all patients were managed clinically by a small group of physicians at Stanford Medical Center. Biopsies were processed into single-cell suspension and stored as live cells in liquid nitrogen. Training and testing patient cohorts were generated by randomly selecting patients to form two sets balanced for age, sex, FLIPI (32), BCR isotype of Igγ or Igμ, and overall survival (Table S2). Investigators were blind to the clinical outcome of patients while quantifying LNP cells in the testing set. Sample collection date and cryopreservation time were equivalent in training and testing sets and were not related to overall survival or biological groupings described. Additional tumor samples studied outside of training and testing sets included posttherapy biopsy specimens (Table S2). All specimens were obtained with informed consent in accordance with the Declaration of Helsinki and this study was approved by Stanford University's Administrative Panels on Human Subjects in Medical Research.

After thawing a sample, 5 million cells were used for flow cytometry–based live/dead discrimination and immunophenotyping (Fig. 1 and Table S3). Signaling was analyzed in the remaining sample using phospho-specific flow cytometry signaling profiles, as outlined in Fig. 1 and as previously described (1, 22, 37). A list of signaling inputs, antibodies, and a detailed protocol are included in *SI Materials and Methods*. Basal levels of signaling were used to examine constitutive or tonic BCR signaling. The BCR signaling response was calculated as fold induction of signaling over basal level. Estimates of survival were calculated using the Kaplan-Meier method with a log-rank test of significance. Analysis of LNP cells as a continuous variable used Cox proportional-hazards regression to model annual average risk of death.

1. Irish JM, et al. (2004) Single cell profiling of potentiated phospho-protein networks in cancer cells. *Cell* 118:217–228.
2. Kotecha N, et al. (2008) Single-cell profiling identifies aberrant STAT5 activation in myeloid malignancies with specific clinical and biologic correlates. *Cancer Cell* 14:335–343.
3. Gupta PB, Chaffer CL, Weinberg RA (2009) Cancer stem cells: Mirage or reality? *Nat Med* 15:1010–1012.
4. Reya T, Morrison SJ, Clarke MF, Weissman IL (2001) Stem cells, cancer, and cancer stem cells. *Nature* 414:105–111.
5. Horning SJ, Rosenberg SA (1984) The natural history of initially untreated low-grade non-Hodgkin's lymphomas. *N Engl J Med* 311:1471–1475.
6. Hanahan D, Weinberg RA (2000) The hallmarks of cancer. *Cell* 100:57–70.
7. Martin GS (2003) Cell signaling and cancer. *Cancer Cell* 4:167–174.
8. Dave SS, et al. (2004) Prediction of survival in follicular lymphoma based on molecular features of tumor-infiltrating immune cells. *N Engl J Med* 351:2159–2169.
9. Glas AM, et al. (2007) Gene-expression and immunohistochemical study of specific T-cell subsets and accessory cell types in the transformation and prognosis of follicular lymphoma. *J Clin Oncol* 25:390–398.
10. Niiro H, Clark EA (2002) Regulation of B-cell fate by antigen-receptor signals. *Nat Rev Immunol* 2:945–956.
11. Reth M, Brummer T (2004) Feedback regulation of lymphocyte signalling. *Nat Rev Immunol* 4:269–277.
12. Kurosaki T, Shinohara H, Baba Y (2010) B cell signaling and fate decision. *Annu Rev Immunol* 28:21–55.
13. Chen L, et al. (2008) SYK-dependent tonic B-cell receptor signaling is a rational treatment target in diffuse large B-cell lymphoma. *Blood* 111:2230–2237.
14. Stevenson FK, Caligaris-Cappio F (2004) Chronic lymphocytic leukemia: Revelations from the B-cell receptor. *Blood* 103:4389–4395.
15. Küppers R (2005) Mechanisms of B-cell lymphoma pathogenesis. *Nat Rev Cancer* 5:251–262.
16. Gururajan M, Jennings CD, Bondada S (2006) Cutting edge: constitutive B cell receptor signaling is critical for basal growth of B lymphoma. *J Immunol* 176:5715–5719.
17. Zhu D, et al. (2002) Acquisition of potential N-glycosylation sites in the immunoglobulin variable region by somatic mutation is a distinctive feature of follicular lymphoma. *Blood* 99:2562–2568.
18. Lam KP, Kühn R, Rajewsky K (1997) In vivo ablation of surface immunoglobulin on mature B cells by inducible gene targeting results in rapid cell death. *Cell* 90:1073–1083.
19. Srinivasan L, et al. (2009) PI3 kinase signals BCR-dependent mature B cell survival. *Cell* 139:573–586.
20. Ruiz-Vela A, et al. (2008) Lentiviral (HIV)-based RNA interference screen in human B-cell receptor regulatory networks reveals MCL1-induced oncogenic pathways. *Blood* 111:1665–1676.
21. Brás A, Ruiz-Vela A, González de Buitrago G, Martinez-A C (1999) Caspase activation by BCR cross-linking in immature B cells: Differential effects on growth arrest and apoptosis. *FASEB J* 13:931–944.
22. Irish JM, Czerwinski DK, Nolan GP, Levy R (2006) Altered B-cell receptor signaling kinetics distinguish human follicular lymphoma B cells from tumor-infiltrating nonmalignant B cells. *Blood* 108:3135–3142.
23. Ngan BY, Chen-Levy Z, Weiss LM, Warnke RA, Cleary ML (1988) Expression in non-Hodgkin's lymphoma of the bcl-2 protein associated with the t(14;18) chromosomal translocation. *N Engl J Med* 318:1638–1644.
24. Silva CM (2004) Role of STATs as downstream signal transducers in Src family kinase-mediated tumorigenesis. *Oncogene* 23:8017–8023.
25. Downward J (2003) Targeting RAS signalling pathways in cancer therapy. *Nat Rev Cancer* 3:11–22.
26. Vivanco I, Sawyers CL (2002) The phosphatidylinositol 3-kinase AKT pathway in human cancer. *Nat Rev Cancer* 2:489–501.
27. Karin M, Greten FR (2005) NF-kappaB: linking inflammation and immunity to cancer development and progression. *Nat Rev Immunol* 5:749–759.
28. Calò V, et al. (2003) STAT proteins: From normal control of cellular events to tumorigenesis. *J Cell Physiol* 197:157–168.
29. Sachs K, Perez O, Pe'er D, Lauffenburger DA, Nolan GP (2005) Causal protein-signaling networks derived from multiparameter single-cell data. *Science* 308:523–529.
30. Janes KA, et al. (2006) The response of human epithelial cells to TNF involves an inducible autocrine cascade. *Cell* 124:1225–1239.
31. Bagley CM, Jr, Devita VT, Jr, Berard CW, Canellos GP (1972) Advanced lymphosarcoma: Intensive cyclical combination chemotherapy with cyclophosphamide, vincristine, and prednisone. *Ann Intern Med* 76:227–234.
32. Solal-Céligny P, et al. (2004) Follicular lymphoma international prognostic index. *Blood* 104:1258–1265.
33. Hikida M, et al. (2009) PLC-gamma2 is essential for formation and maintenance of memory B cells. *J Exp Med* 206:681–689.
34. Chen L, et al. (2008) SYK-dependent tonic B-cell receptor signaling is a rational treatment target in diffuse large B-cell lymphoma. *Blood* 111:2230–2237.
35. Harris NL, et al. (1994) A revised European-American classification of lymphoid neoplasms: A proposal from the International Lymphoma Study Group. *Blood* 84:1361–1392.
36. Meeker T, et al. (1985) Emergence of idiotype variants during treatment of B-cell lymphoma with anti-idiotype antibodies. *N Engl J Med* 312:1658–1665.
37. Irish JM, Czerwinski DK, Nolan GP, Levy R (2006) Kinetics of B cell receptor signaling in human B cell subsets mapped by phosphospecific flow cytometry. *J Immunol* 177:1581–1589.
38. Reth M (2002) Hydrogen peroxide as second messenger in lymphocyte activation. *Nat Immunol* 3:1129–1134.
39. Singh DK, et al. (2005) The strength of receptor signaling is centrally controlled through a cooperative loop between Ca2+ and an oxidant signal. *Cell* 121:281–293.
40. Chen L, Juszczynski P, Takeyama K, Aguiar RC, Shipp MA (2006) Protein tyrosine phosphatase receptor-type O truncated (PTPROt) regulates SYK phosphorylation, proximal B-cell-receptor signaling, and cellular proliferation. *Blood* 108:3428–3433.
41. Braselmann S, et al. (2006) R406, an orally available spleen tyrosine kinase inhibitor blocks fc receptor signaling and reduces immune complex-mediated inflammation. *J Pharmacol Exp Ther* 319:998–1008.
42. Kawabe T, et al. (1994) The immune responses in CD40-deficient mice: impaired immunoglobulin class switching and germinal center formation. *Immunity* 1:167–178.
43. Mizuno T, Rothstein TL (2005) B cell receptor (BCR) cross-talk: CD40 engagement creates an alternate pathway for BCR signaling that activates I kappa B kinase/I kappa B alpha/NF-kappa B without the need for PI3K and phospholipase C gamma. *J Immunol* 174:6062–6070.
44. Wheeler K, Pound JD, Gordon J, Jefferis R (1993) Engagement of CD40 lowers the threshold for activation of resting B cells via antigen receptor. *Eur J Immunol* 23:1165–1168.
45. Maloney DG, et al. (1997) IDEC-C2B8 (Rituximab) anti-CD20 monoclonal antibody therapy in patients with relapsed low-grade non-Hodgkin's lymphoma. *Blood* 90:2188–2195.
46. Marcus R, et al. (2008) Phase III study of R-CVP compared with cyclophosphamide, vincristine, and prednisone alone in patients with previously untreated advanced follicular lymphoma. *J Clin Oncol* 26:4579–4586.
47. Hochster H, et al. (2009) Maintenance rituximab after cyclophosphamide, vincristine, and prednisone prolongs progression-free survival in advanced indolent lymphoma: Results of the randomized phase III ECOG1496 Study. *J Clin Oncol* 27:1607–1614.
48. Johnson NA, et al. (2009) Diffuse large B-cell lymphoma: Reduced CD20 expression is associated with an inferior survival. *Blood* 113:3773–3780.
49. Bahler DW, Levy R (1992) Clonal evolution of a follicular lymphoma: Evidence for antigen selection. *Proc Natl Acad Sci USA* 89:6770–6774.
50. Zelenetz AD, Chen TT, Levy R (1992) Clonal expansion in follicular lymphoma occurs subsequent to antigenic selection. *J Exp Med* 176:1137–1148.
51. Radcliffe CM, et al. (2007) Human follicular lymphoma cells contain oligomannose glycans in the antigen-binding site of the B-cell receptor. *J Biol Chem* 282:7405–7415.